

# Timescales of electrons wave-particle interactions with chorus and hiss in the outer radiation belts

Oleksiy Agapitov<sup>1</sup>, Didier Mourenas<sup>2</sup>, Anton Artemyev<sup>3</sup>, Forrest Mozer<sup>1</sup>, and John Bonnell<sup>1</sup>

<sup>1</sup> *Space Science Laboratory, University of California, Berkeley, Berkeley, CA*

<sup>2</sup> *CEA, DAM, DIF, Arpajon, France*

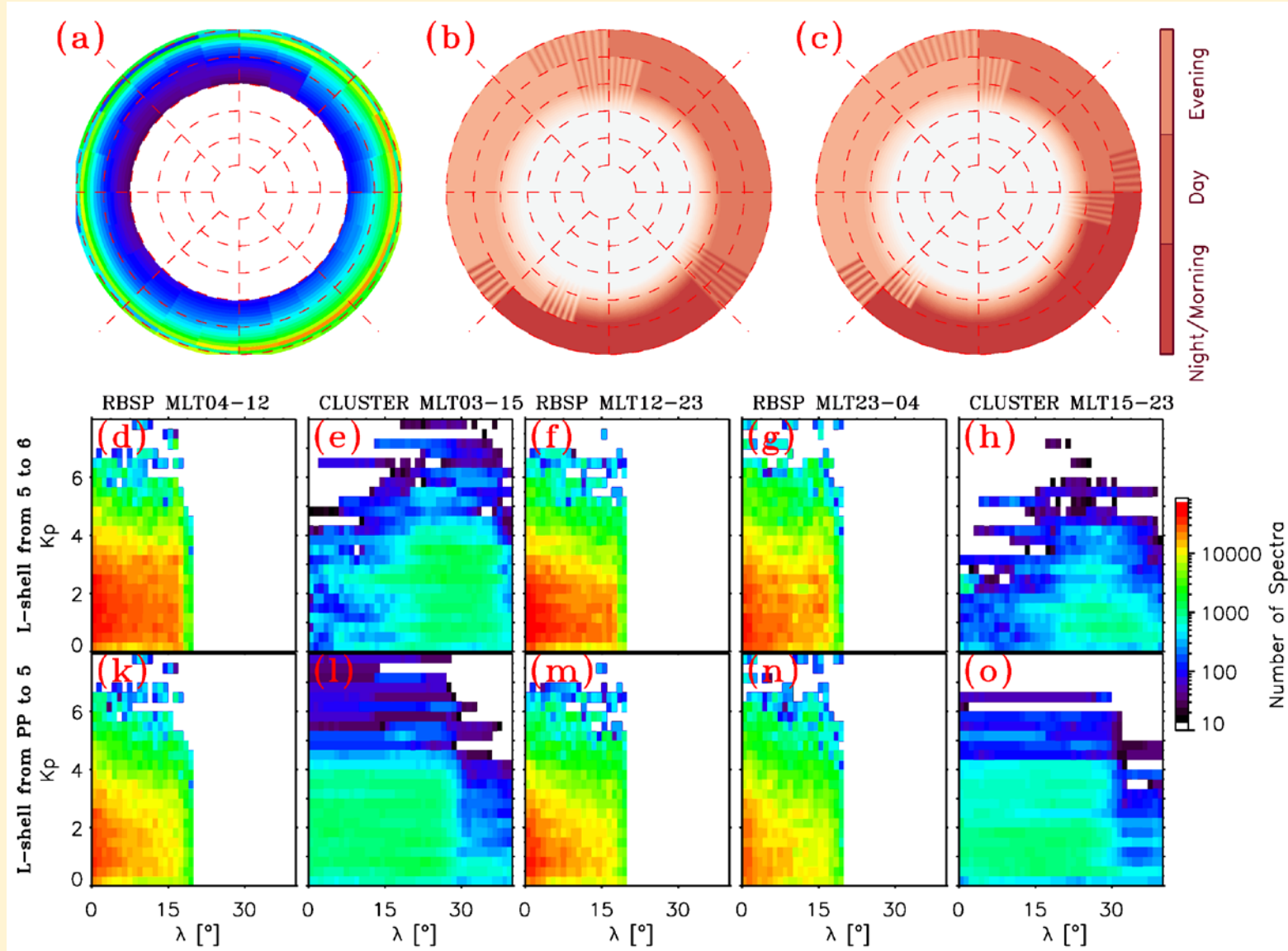
<sup>3</sup> *University of California, Los Angeles, Los Angeles, CA*

[agapitov@ssl.berkeley.edu](mailto:agapitov@ssl.berkeley.edu)

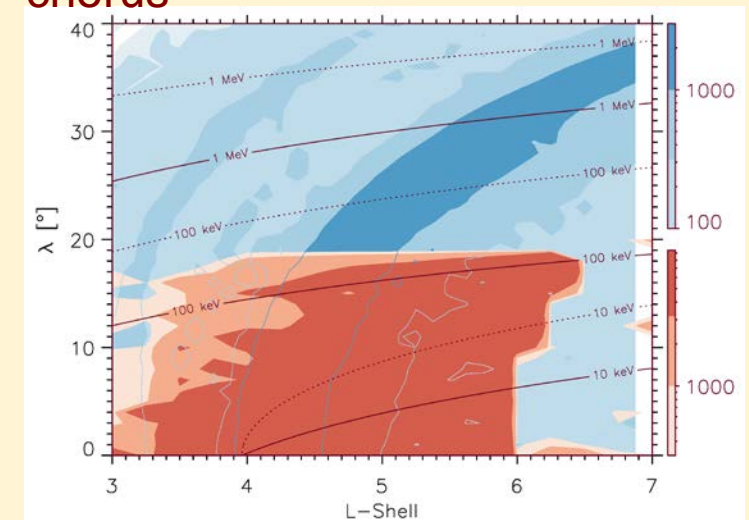
The factors recently highlighted by Van Allen Probes to affect the efficiency and control the predominance of the precipitation or acceleration regimes by chorus and hiss to be included into the long scale wave-particle interaction models:

- **whistler-mode wave amplitude distribution with latitude** determines the regime of scattering or acceleration;
- **wave normal angle distribution:** existence of the significant oblique whistler population's influence on electron scattering;
- **chorus frequency dependence on latitude** was supposed to be constant, however, *Van Allen Probes* showed that the relative wave frequency goes down with latitude from  $0.35 f_{ce}$  at the equator to  $\sim 0.1 f_{ce}$  at 20 degrees, decreasing the electron scattering resonance latitude from  $\sim 30$  degrees to  $\sim 15$  degrees;
- **$\omega_{pe}/\Omega_{ce}$  value affects the energy and pitch-angle scattering rates and also sufficiently influences the electron scattering resonance latitudes.**

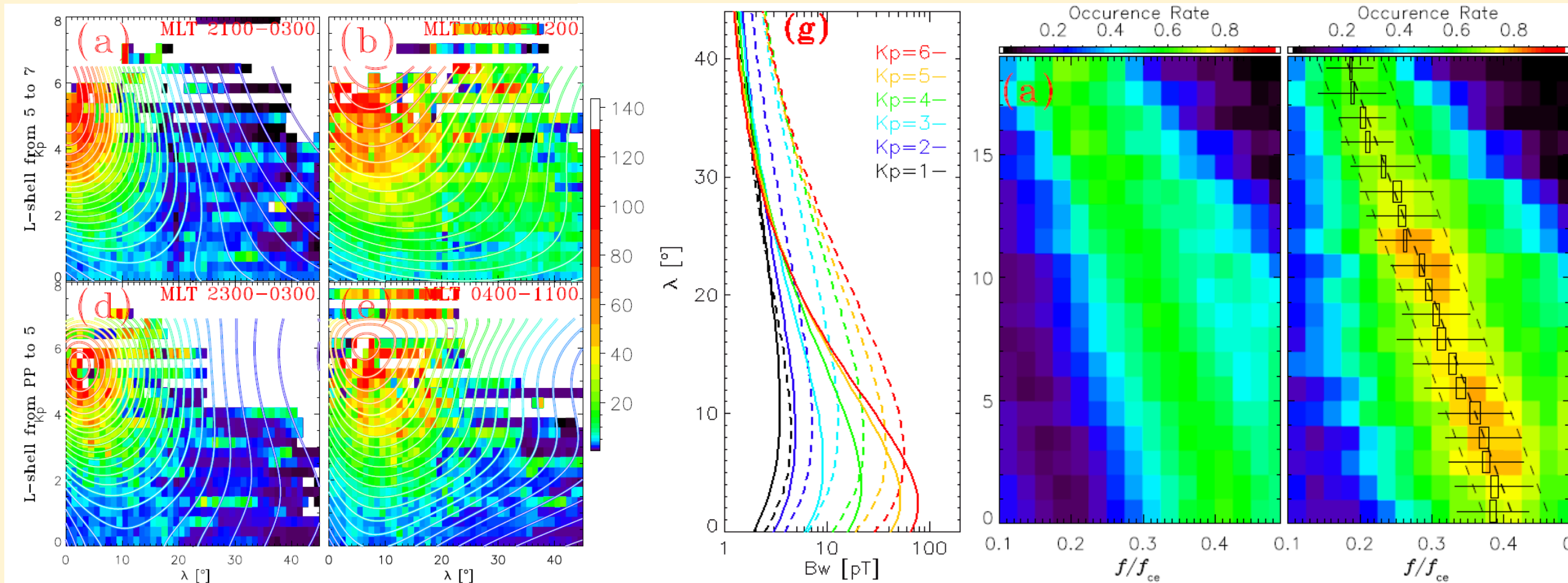
# The chorus model



Data coverage of at  $L = 4-6$  from EMFISIS aboard the Van Allen Probes in 2012-2016 (a) and from CLUSTER STAFF-SA during 2001-2010 in the chorus frequency range ( $0.1f_{ce} < f < f_{ce}$ ), given as the number of spectra captured in  $\lambda$ - $K_p$  domain for day/night sector and two L-shell ranges. Location of cyclotron resonances for quasi-parallel chorus

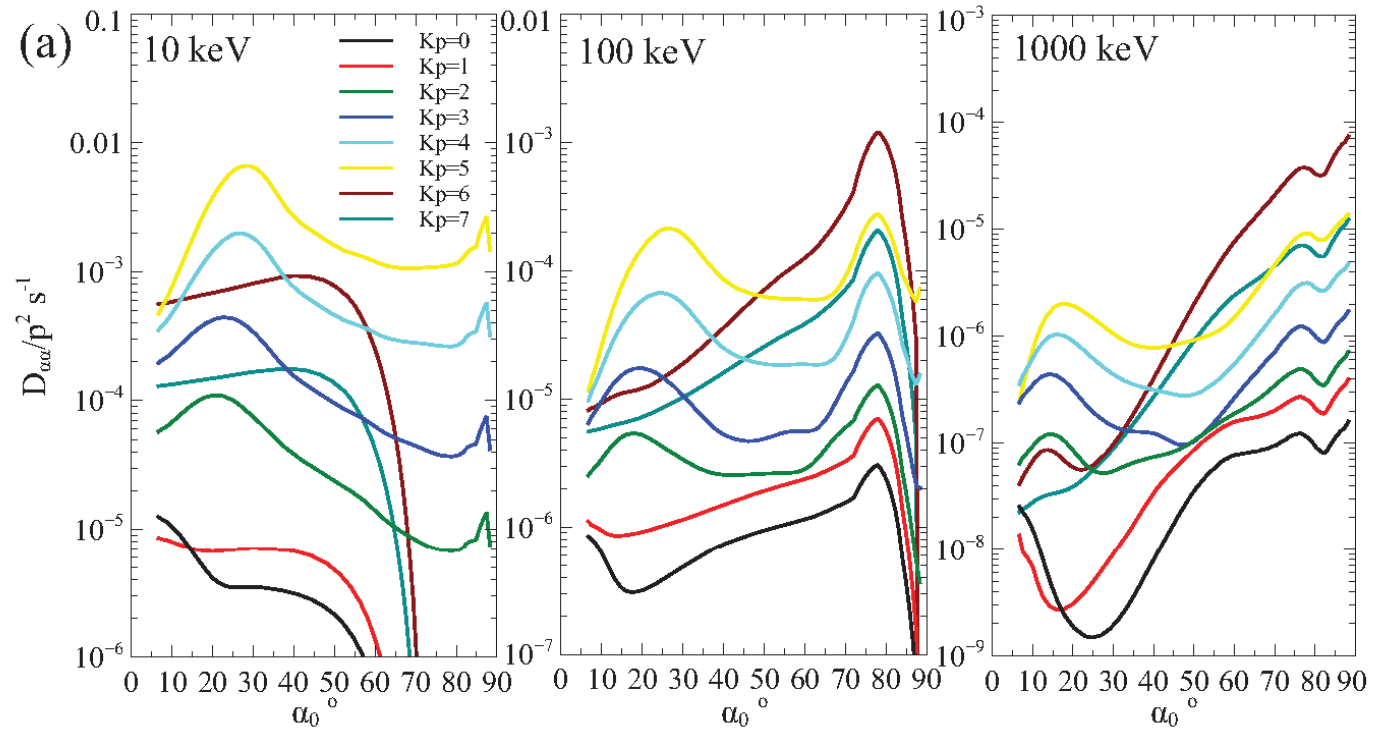
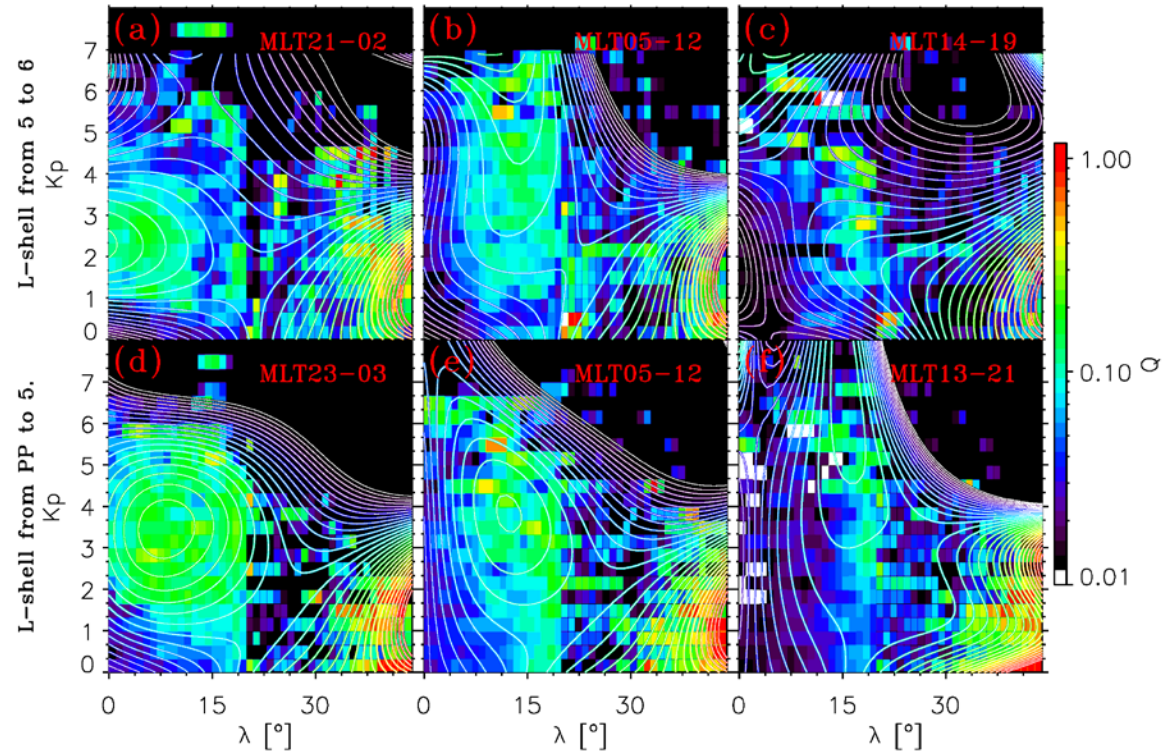


# The chorus model



RMS chorus amplitude profiles in the day and night-morning sectors from the model by Agapitov et al. (2018) for the day (dashed curves) and night-morning (solid curves) sectors.

Chorus  $\omega/\Omega_{ce}$  on latitude from RBSP 2012-2016



Distribution of obliquity factor  $Q$  describing the amount of very oblique LB chorus waves based on Van Allen Probes ( $\lambda < 20$ ) and Cluster ( $\lambda > 20$ ) measurements, shown by solid colors for three MLT (indicated in the panels) sectors and two L-shell ranges (Agapitov et al. 2018).

MLT-averaged pitch-angle diffusion rates for three electron energies and (a)  $L = 4:5$  with the  $Q$  model given by Eq. (4), (b)  $L = 4:5$  and  $Q=0$ , (c)  $L = 6:0$  with the  $Q$  model given by Eq. (4), (d)  $L = 6:0$  and  $Q = 0$  (Agapitov et al. 2018).

# Changing the regime of wave-particles interactions

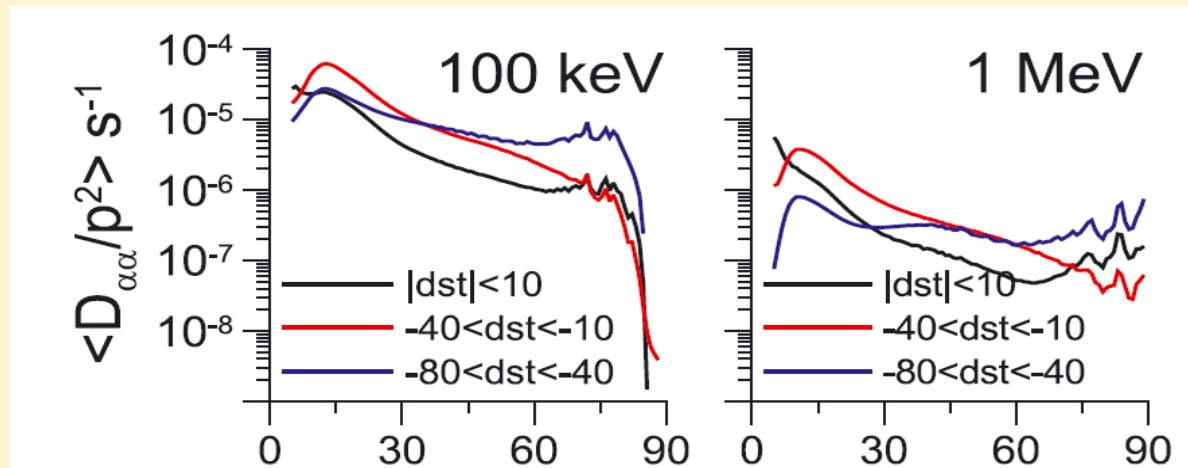
$$D_{\alpha\alpha} \sim B_w^2(\omega)g(\theta)$$

$$D_{EE} \sim B_w^2(\omega)$$

Acceleration efficiency is

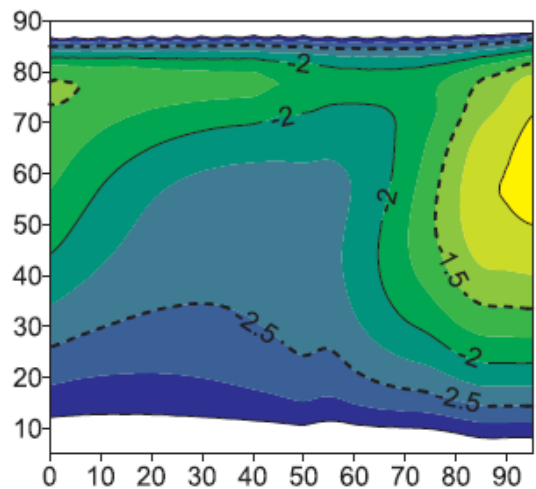
$$\tau_L D_{EE}$$

$\tau_L \sim 1/D_{\alpha\alpha}$  so, does not change with  $B_w$  for purely parallel waves. Taking into account data from Cluster the efficiency of acceleration depends on geomagnetic activity. Efficiency of the acceleration of 100 keV and 1 MeV electrons in dependence on  $D_{st}$  and electron (Artemyev et al., 2016)

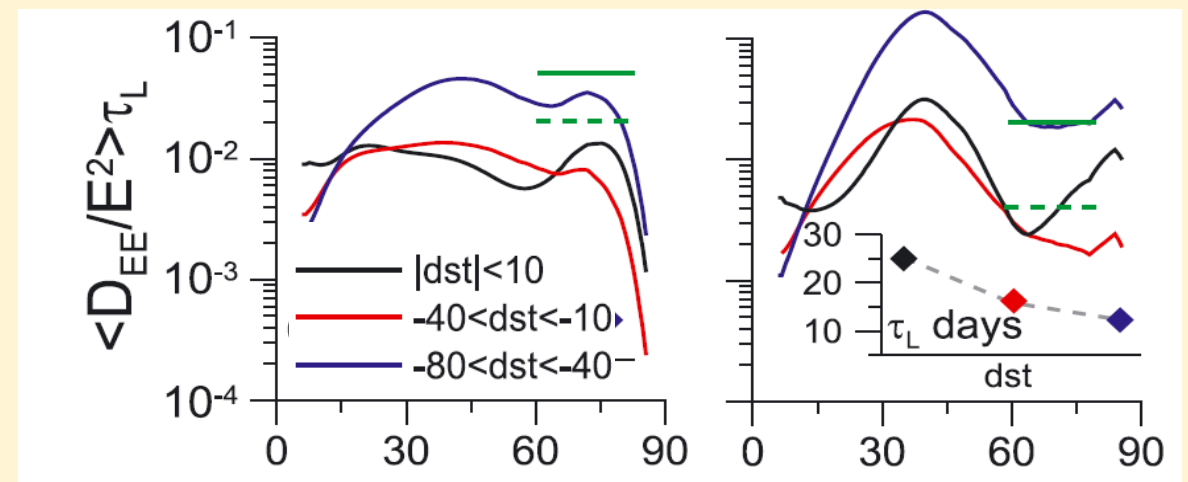
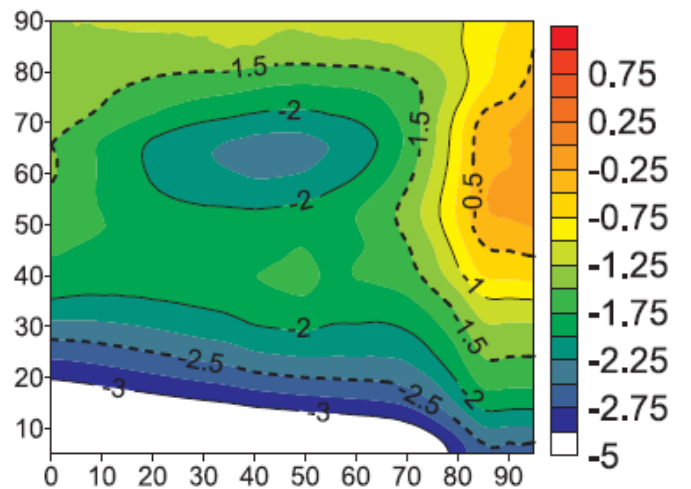


Pitch angle diffusion coefficients for the three  $D_{st}$  ranges and the two energies (Artemyev et al., 2013).

100 keV

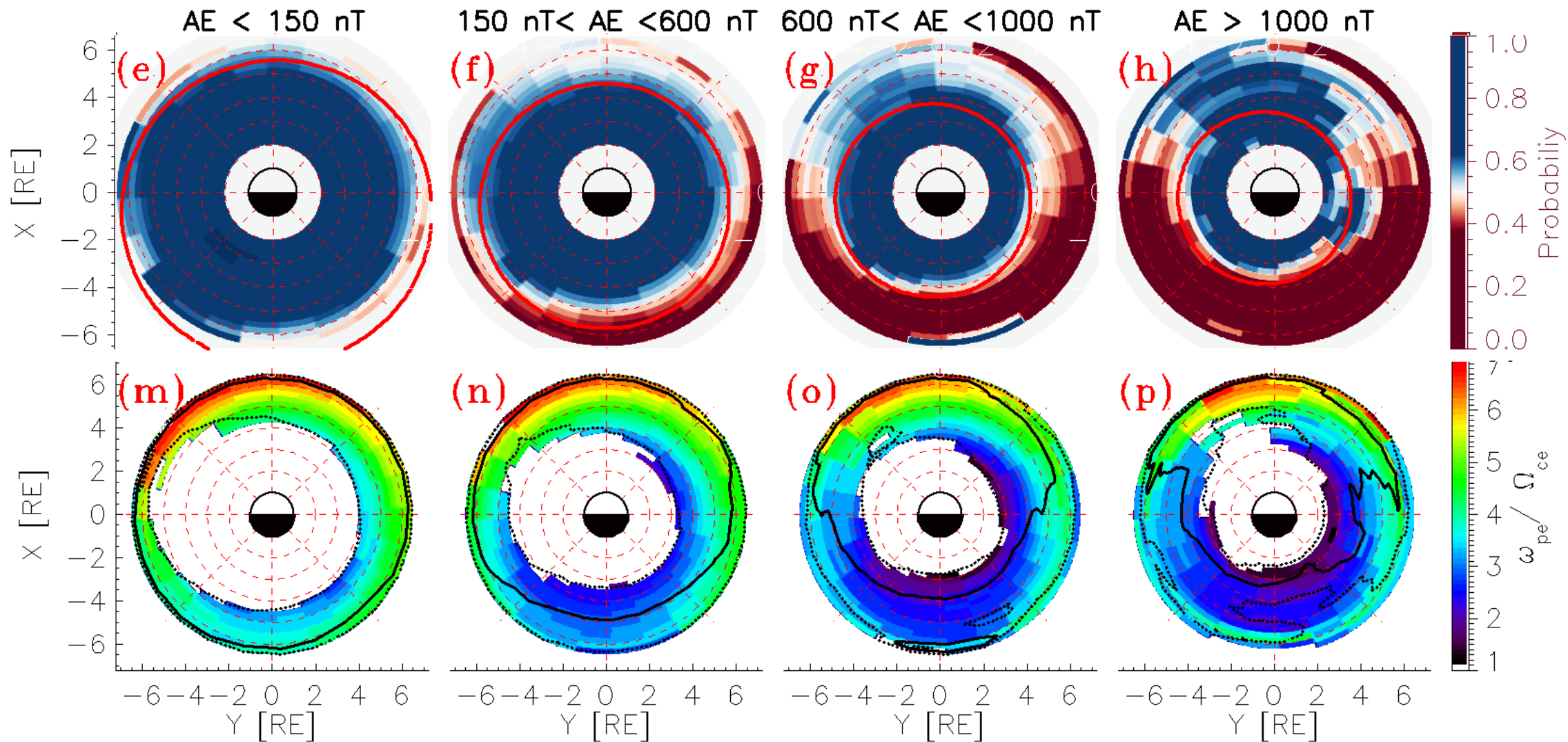


1 MeV  $\log_{10}(\langle D_{EE}/E^2 \rangle \tau_L)$

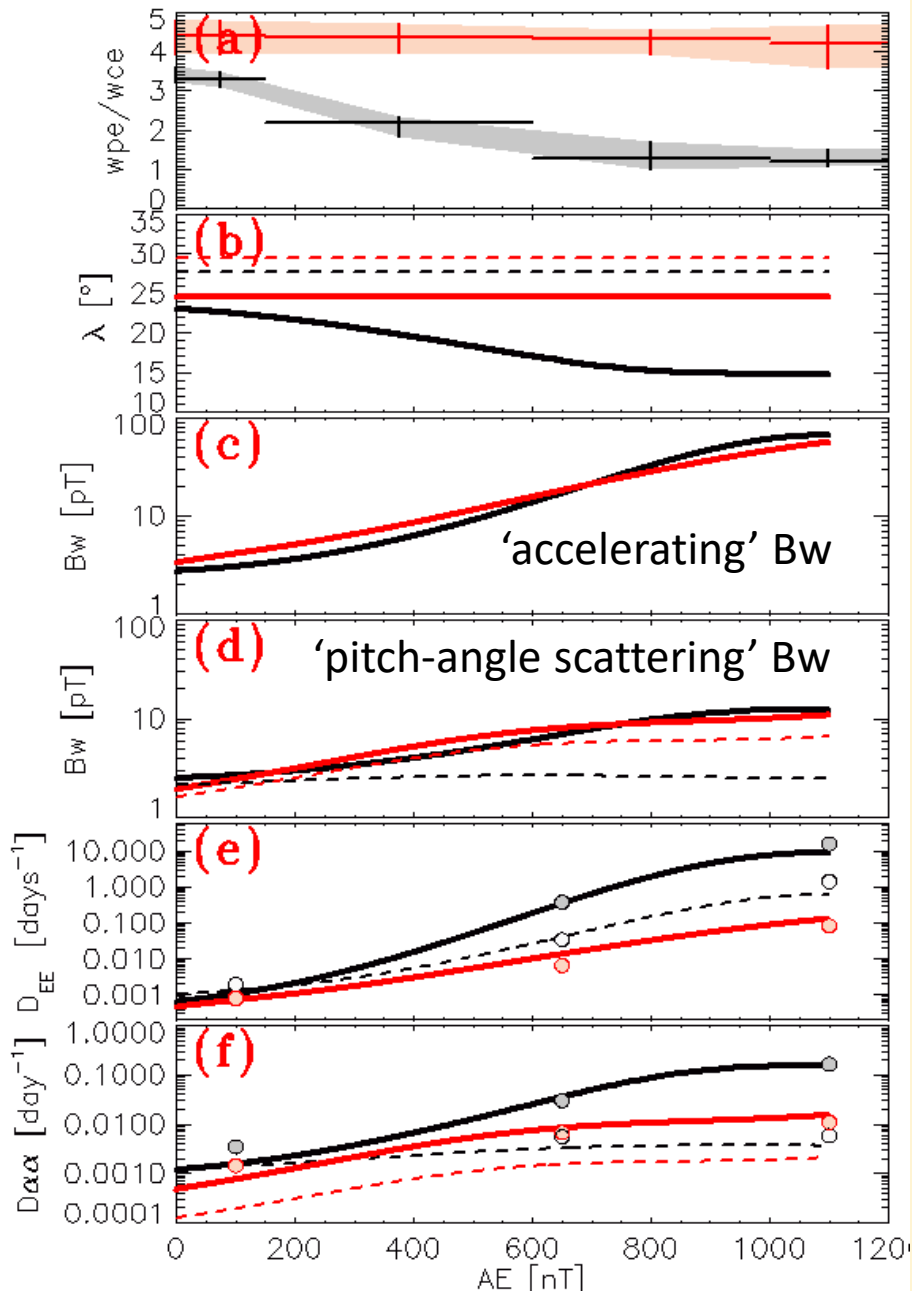


Efficiency of the acceleration: energy diffusion coefficients multiplied on electron lifetime for three  $D_{st}$  ranges and two energies (Artemyev et al., 2013).

# $\omega_{pe}/\Omega_{ce}$ in the plasmasphere and plasma trough



Probability to be inside the plasmasphere from EMFISIS HFR-WFR measurements for the different geomagnetic activity ranges. The solid red curve indicates the model plasmopause by O'Brian and Moldwin (2003).  $\omega_{pe}/\Omega_{ce}$  in the plasma trough for the same geomagnetic activity ranges (Agapitov et al., 2019).

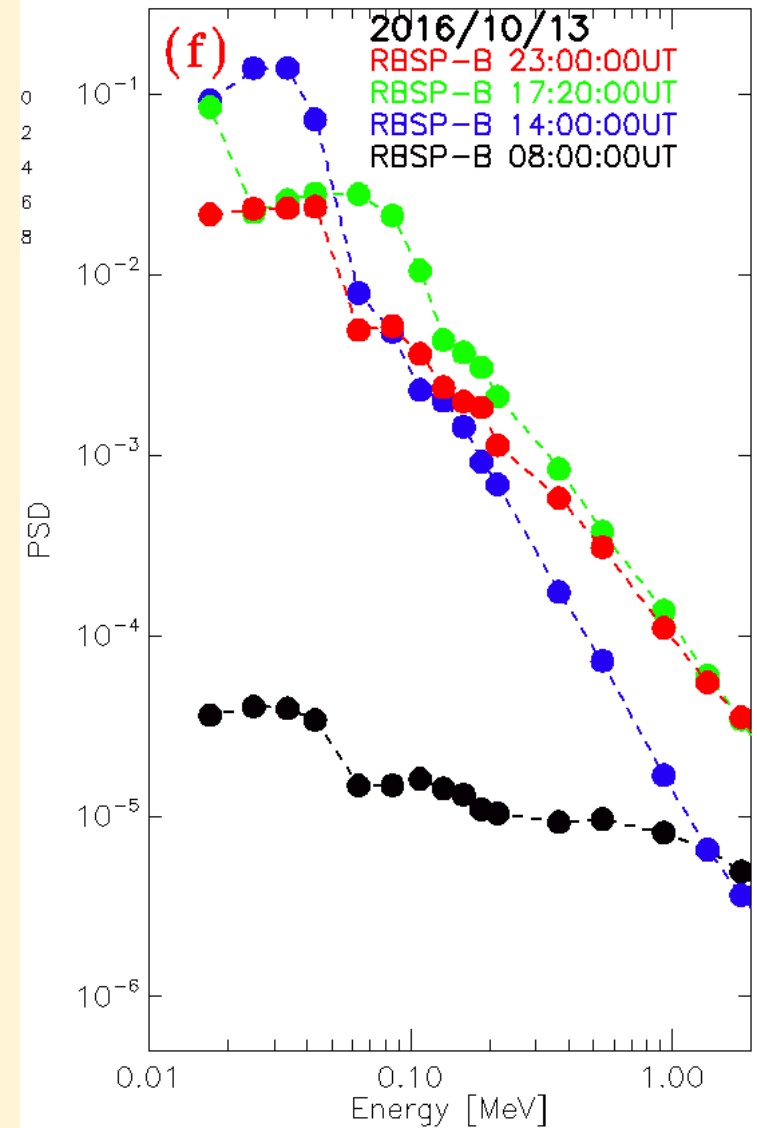
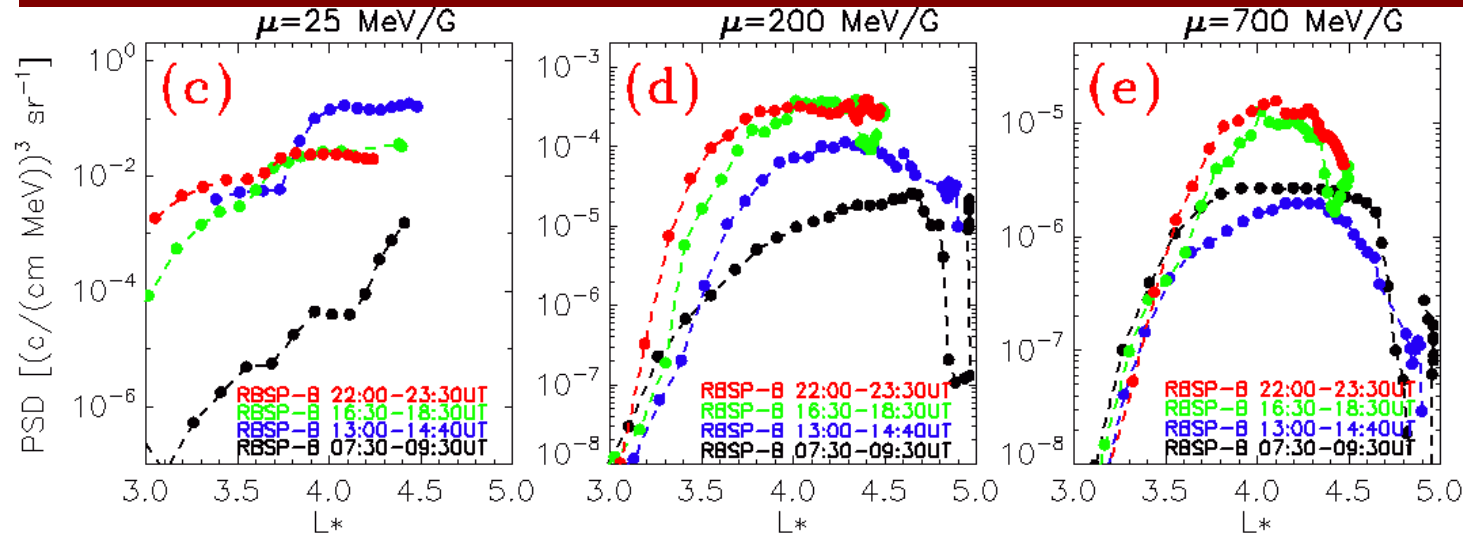


- (a) Variation of  $\omega_{pe}/\Omega_{ce}$  with AE in the day (red) and night (black) sectors;
- (b) Latitude of cyclotron resonance  $\lambda_{R,S}$  with 1 MeV electrons near their loss-cone ( $\lambda_{R,S}$  for constant  $\omega_{pe}/\Omega_{ce}$  values of 4.3 and 3.5 in the day and night sectors, respectively, are shown by dashed lines);
- (c) RMS chorus wave amplitude in the vicinity of the geomagnetic equator, where most of the chorus-driven electron energization occurs;
- (d) RMS chorus wave amplitude at  $\lambda_{R,S}$  (for 1 MeV electrons) where chorus-driven scattering leads to precipitation in the atmosphere;
- (e) chorus-driven energy scattering rate  $D_{EE}$  for measured  $\omega_m/\Omega_{ce}$ ,  $\omega_{pe}/\Omega_{ce}$  (solid curves), the dotted black curve showing  $D_{EE}$  for a constant  $\omega_{pe}/\Omega_{ce} = 3.5$  in the night sector;
- (f) Same as (e) for the chorus-driven pitch-angle scattering rate  $D_{aa}$  near the loss-cone;

—  $f/f_{ce}$  from RBSP  
—  $\omega_{pe}/\Omega_{ce}$  from RBSP  
—  $f/f_{ce}$  from RBSP  
—  $\omega_{pe}/\Omega_{ce}$  from RBSP

- - -  $f/f_{ce} = 0.35$   
- - -  $\omega_{pe}/\Omega_{ce} = 4.5$   
- - -  $f/f_{ce} = 0.35$   
- - -  $\omega_{pe}/\Omega_{ce} = 3.5$

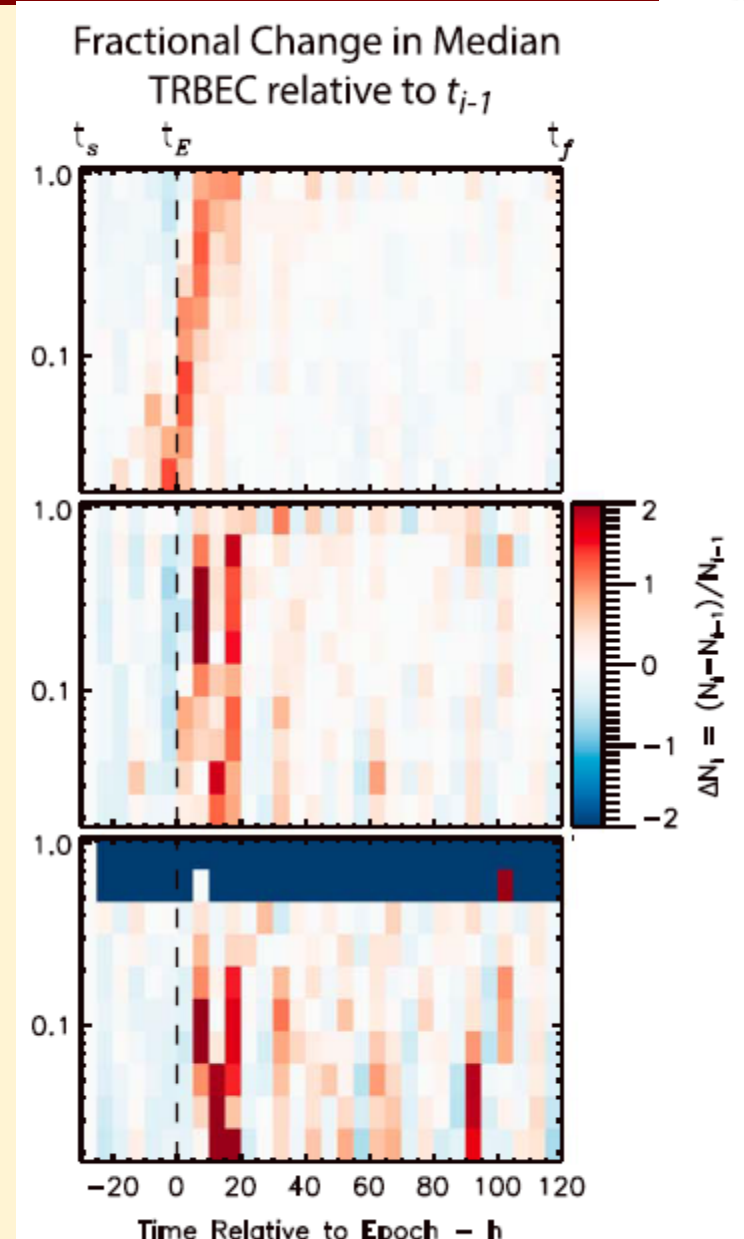
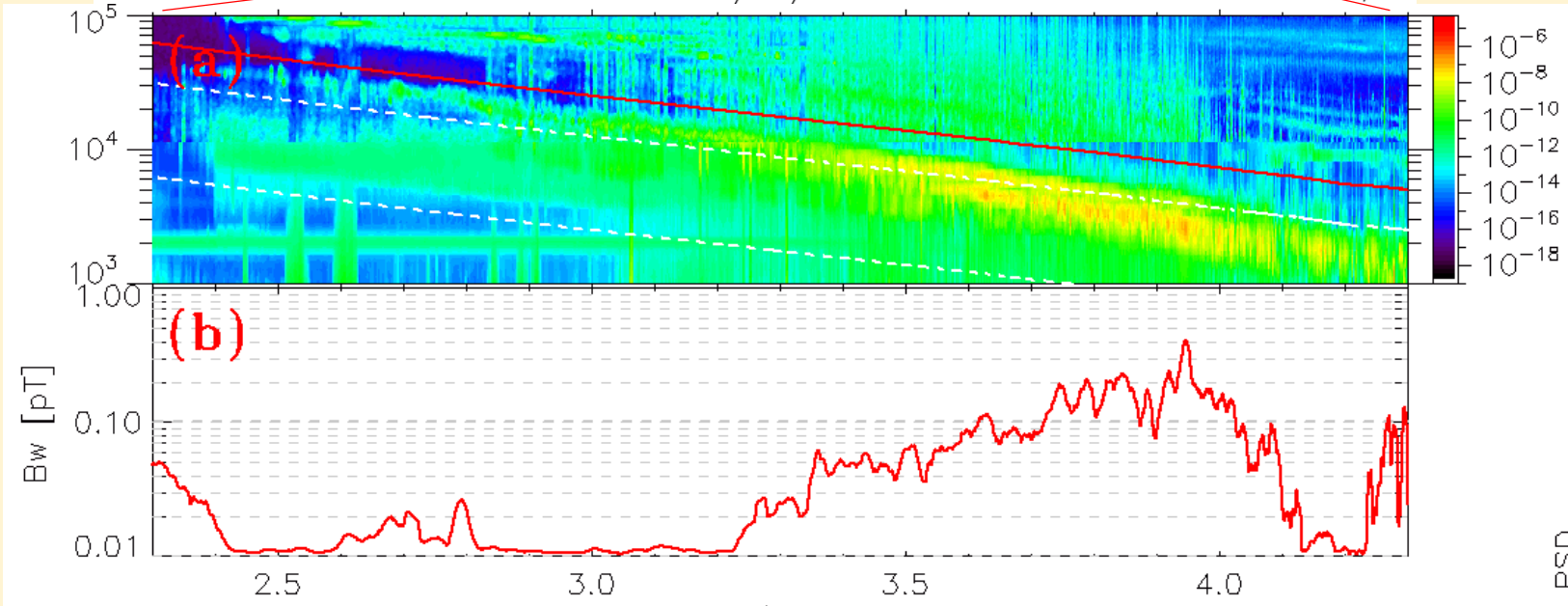
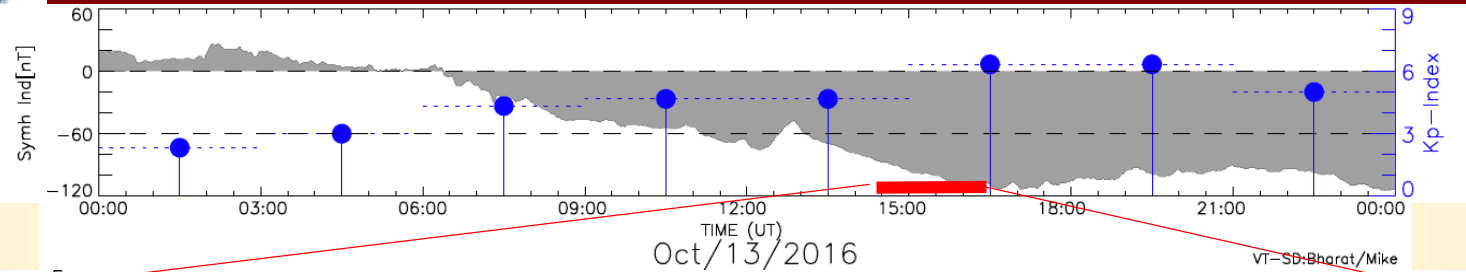
(Agapitov et al., 2019).



The dynamics of electron PSD for  $\mu=25$ , 200 and 700 MeV/G, respectively (corresponding to energies 0.1, 0.6, and 1.4 MeV at  $L^*=4$ ) from Van Allen Probe B. Different colors correspond to different times indicated in the legend of panel (f). Panel (f) shows the dynamics of the electron PSD as a function of electron energy at  $L^*=4$ .

The enhancement of 10-200 keV particles is caused by the injection. The enhancement of 0.5-2 MeV electrons is local with a maximum at  $L^*=4$ . The acceleration time scale can be estimated from the inbound and the following outbound orbits as  $\sim 2$  hours (Agapitov et al., 2019).

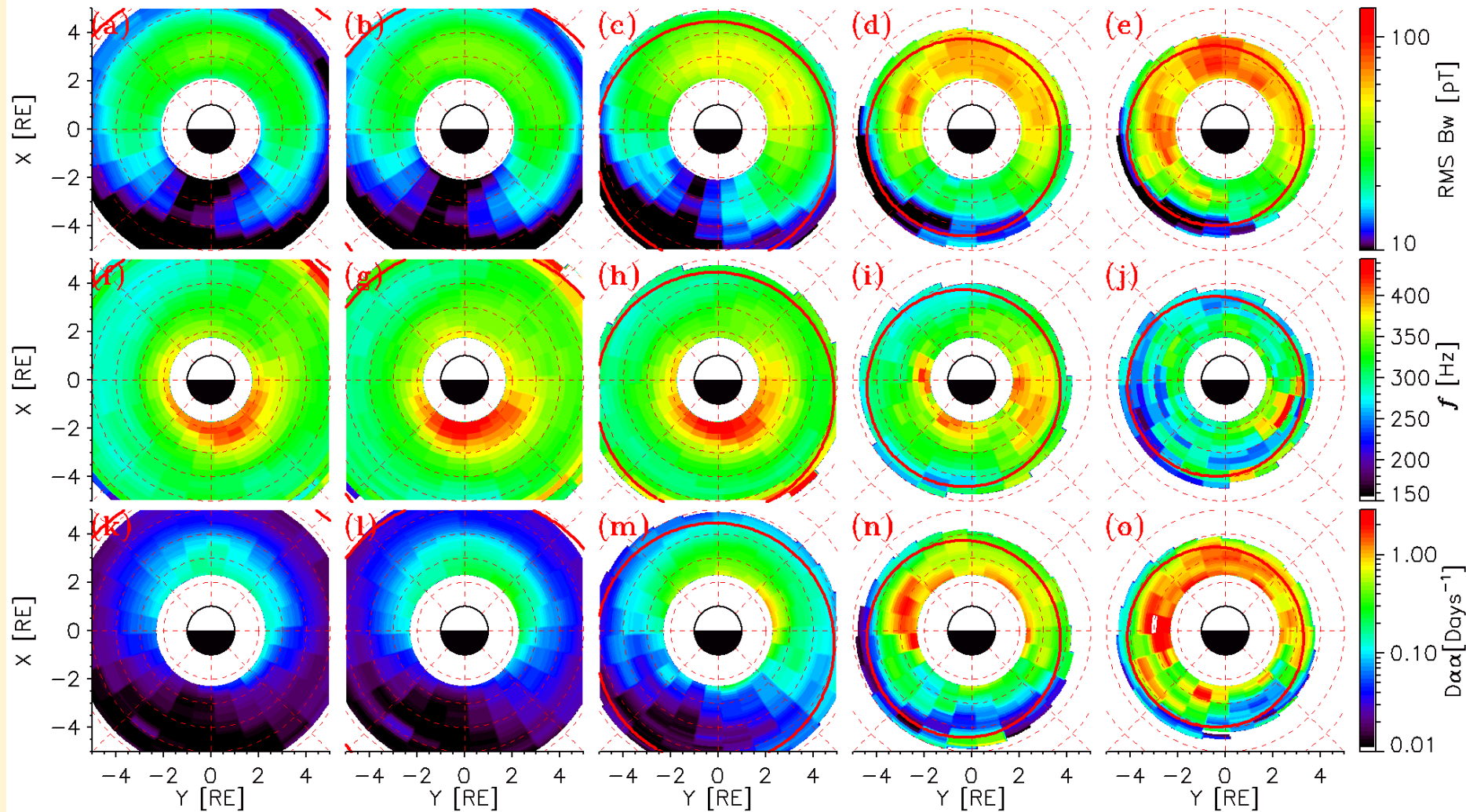
# Wave dynamics and effects for particles



(a) - Dynamic spectrum of chorus wave electric field from Van Allen Probe A, on 2016-10-13 (14:40-16:10UT.  $\omega_{pe}/\Omega_{ce}$  is  $\sim 1.2-1.3$  at 15-16UT. These parameters lead to time scales  $\sim 2$  hours instead of  $\sim 18$  hours.

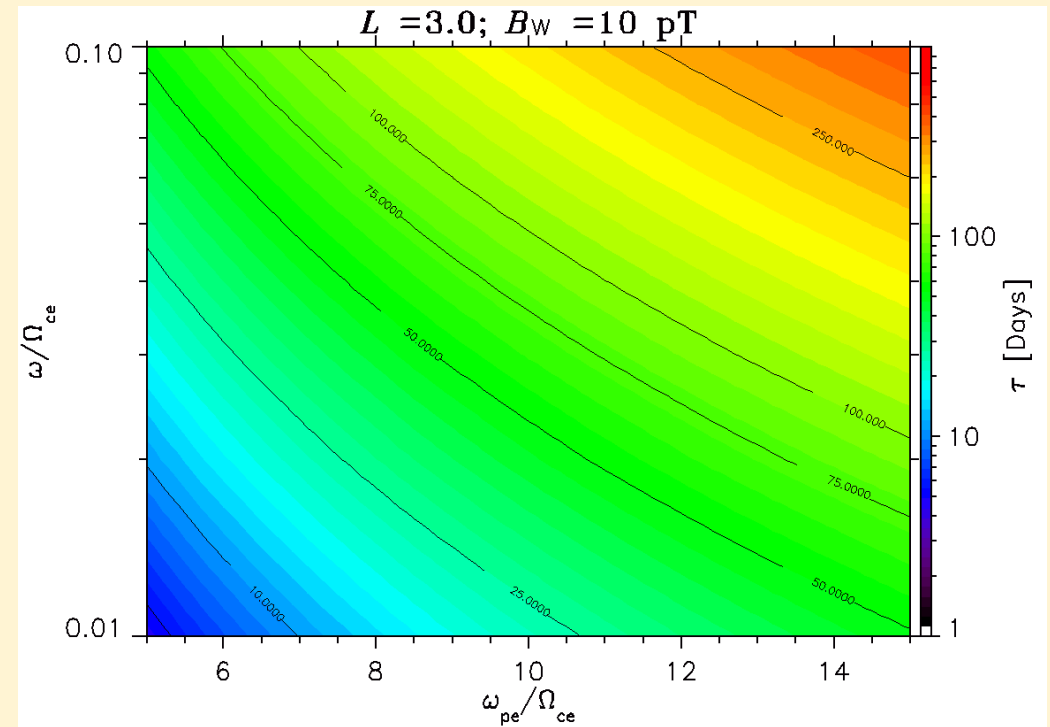
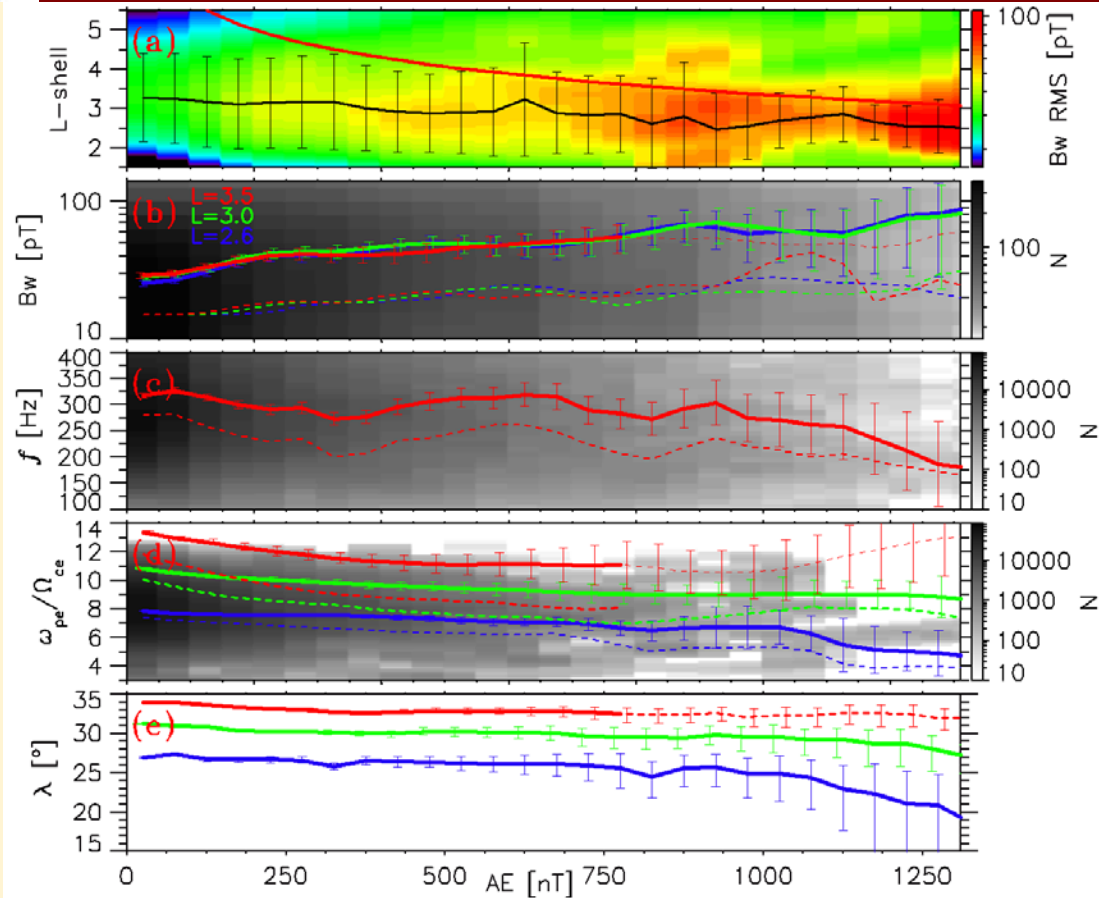
Murphy et al., 2018

# The HISS model

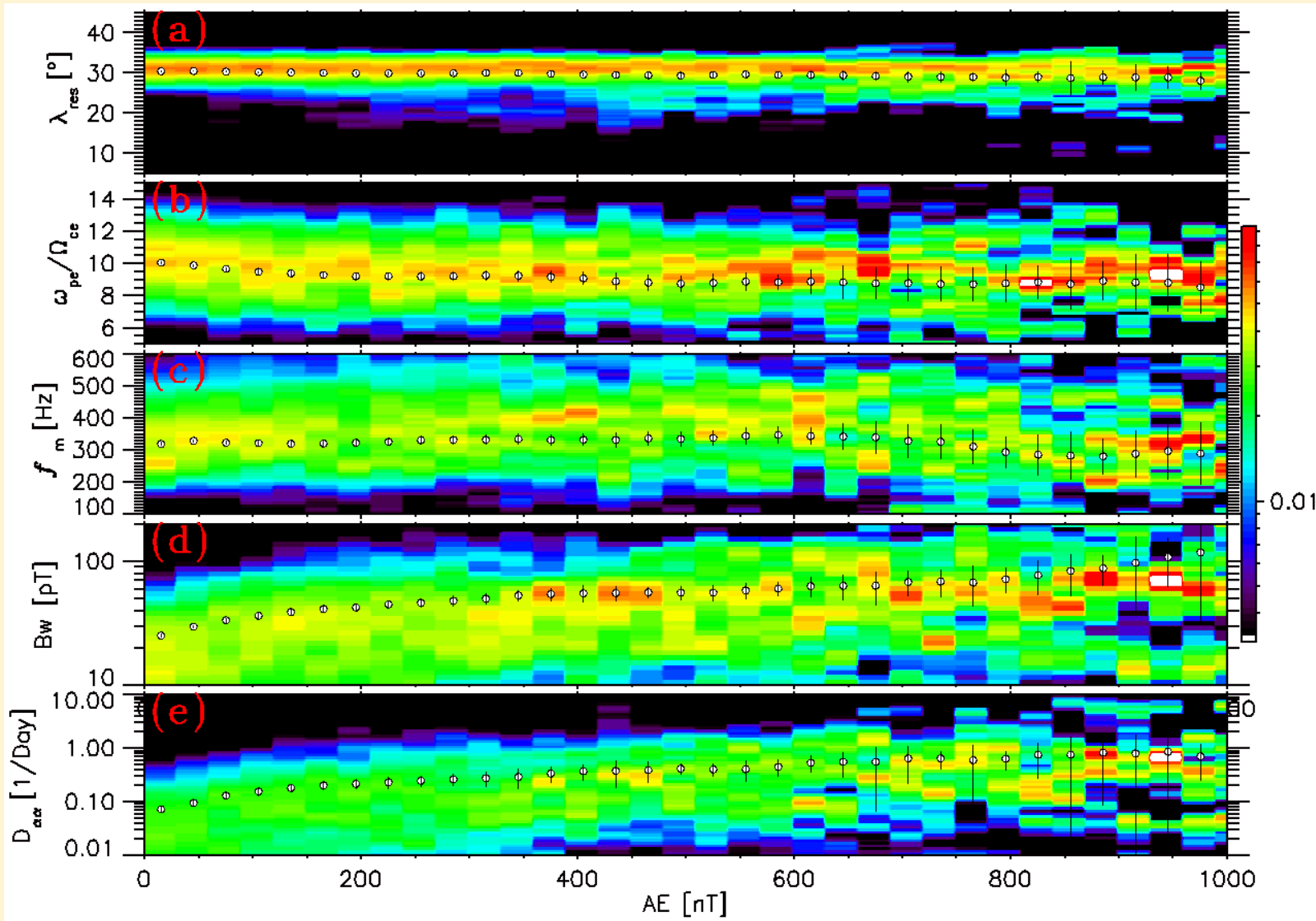


(a-e) Distribution of hiss RMS amplitude  $B_w$  from EMFISIS HFR in the plasmasphere or in plumes, for the same geomagnetic activity levels as in Figure 1. The outer limit of the region of plasmaspheric hiss waves determined by the plasmopause model of O'Brien and Moldwin (2003) is shown by solid red curves. (f-j) Distribution of hiss wave frequency at peak wave amplitude as a function of  $AE$  (Agapitov et al., 2020).

# The HISS model

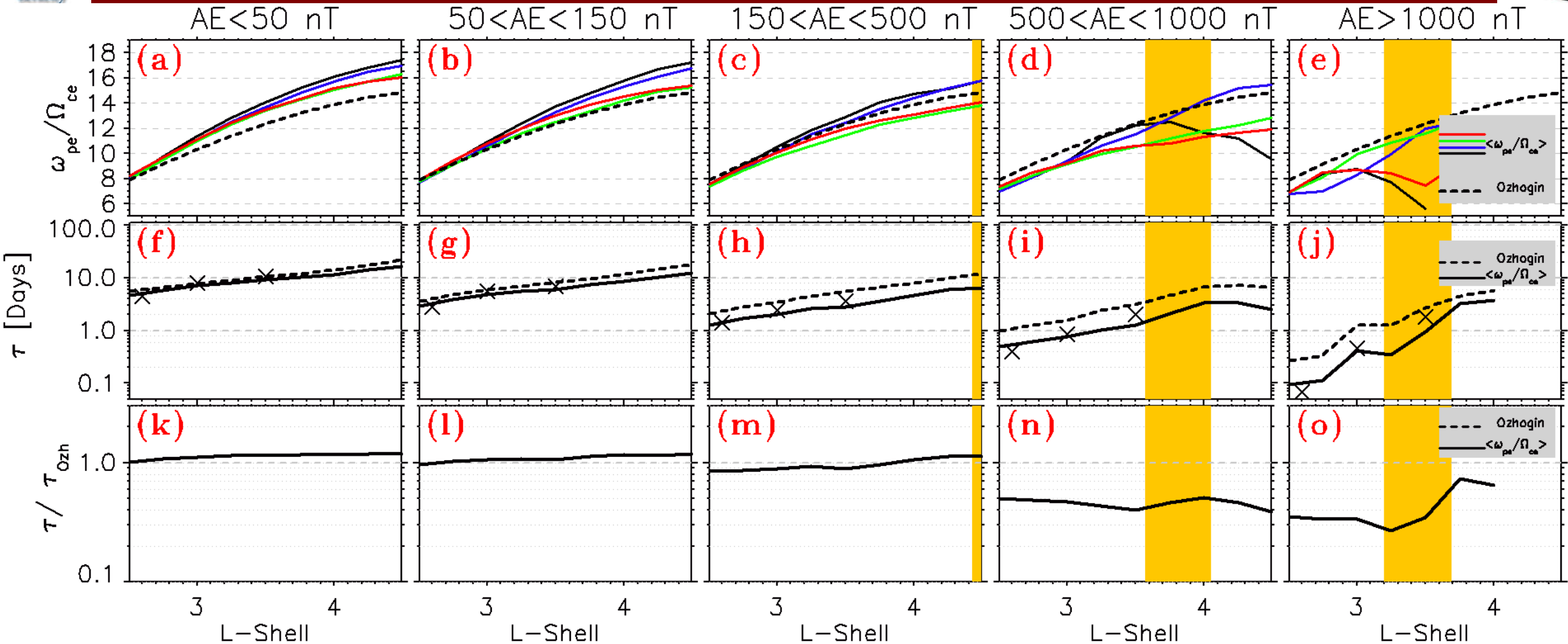


(a) Distribution of hiss wave RMS amplitude with  $L$ -shell. Amplitudes larger than half the maximum are shown by bars. The plasmopause is indicated by a solid red curve. (b) RMS hiss wave power at  $L=2.6$ ,  $3.0$ , and  $3.5$  (the blue, green, red curves respectively). Dotted curves show nightside hiss amplitudes. (c) Hiss wave frequency (weighted by wave power). (d) Mean  $\omega_{pe}/\Omega_{ce}$  at  $L=2.6$  (blue),  $L=3.0$  (green), and  $L=3.5$  (red). (e) Latitude of cyclotron resonance with 1-MeV electrons near the loss-cone (blue),  $L=3.0$  (green), and  $L=3.5$  (red). (f) Lifetime of 1-MeV electrons at  $L = 3.0$  estimated in the  $(\omega_m/\Omega_{ce}, \omega_{pe}/\Omega_{ce})$  domain at  $L=2.6$  (for  $B_w = 10$  pT (Agapitov et al., 2020)).



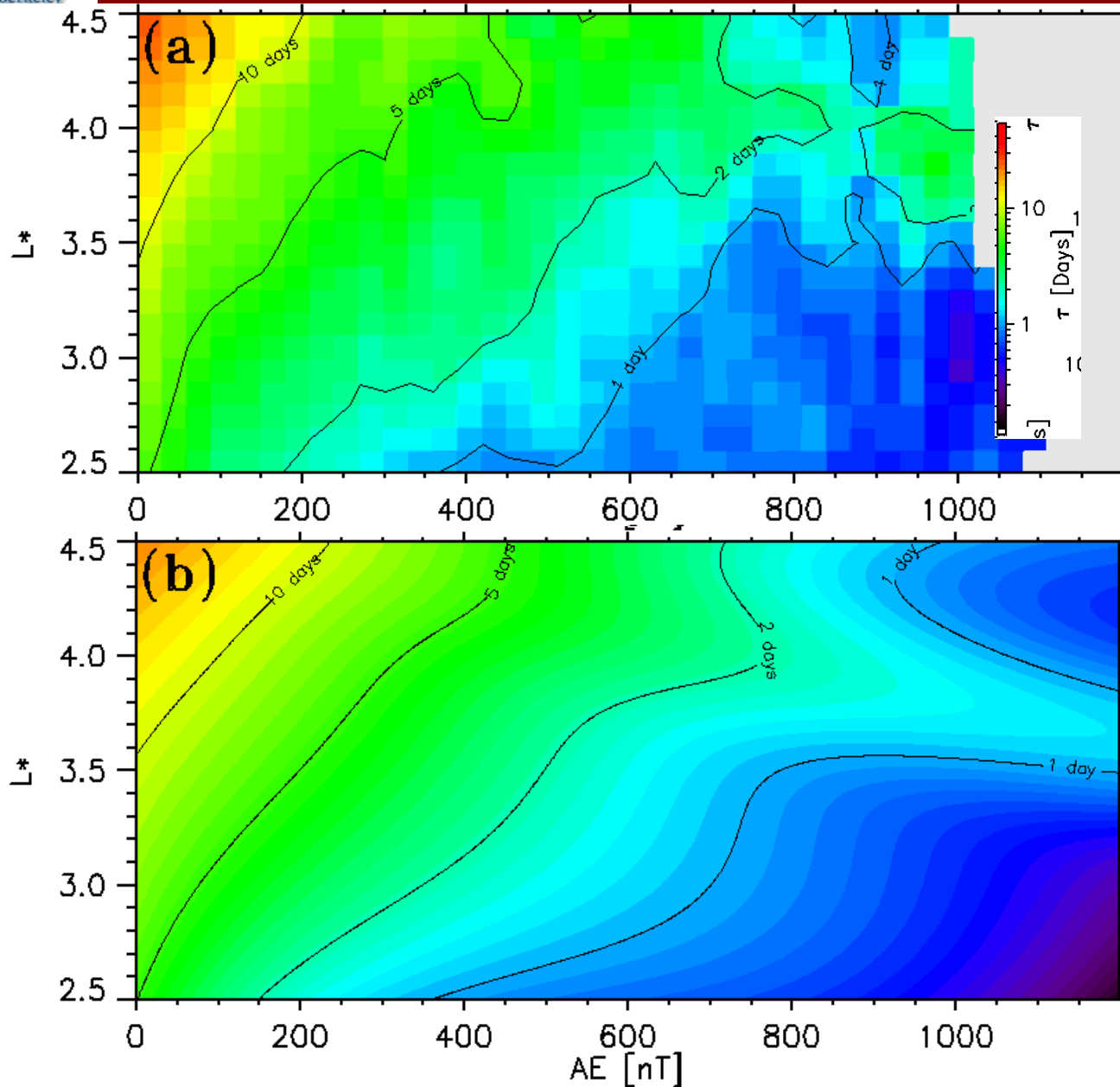
(a) Distribution of latitude for cyclotron resonance between 1-MeV electrons and hiss waves as a function of  $AE$  for  $L = 3$ . (b,c,d) Corresponding simultaneous distributions of  $\omega_{pe}/\Omega_{ce}$ , hiss wave mean frequency (weighted by wave power), and wave amplitude. (e) Corresponding distribution of analytical estimates of bounced-averaged pitch-angle scattering rates. Circles show mean values and bars show the standard deviation (Agapitov et al., 2019).

# The HISS model

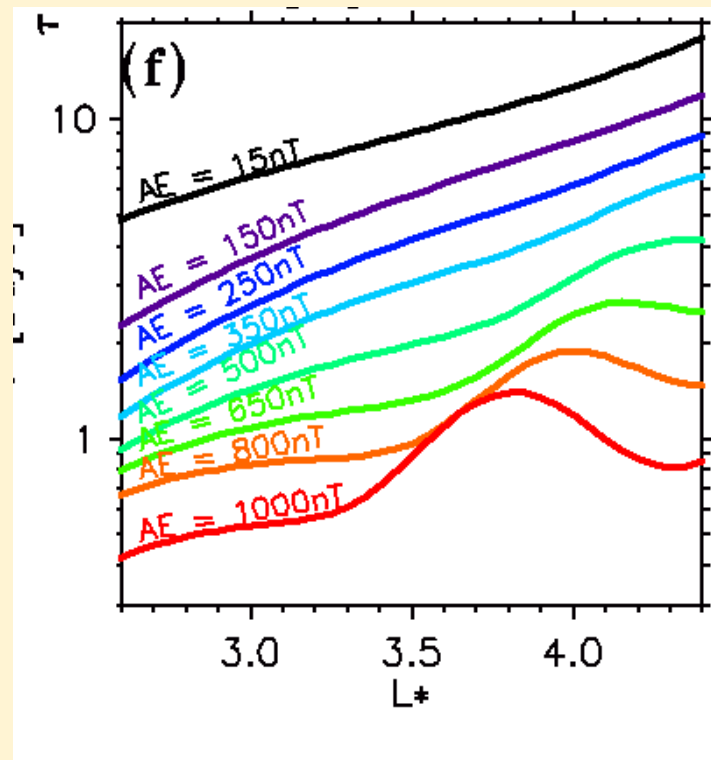


(a-e) Variation of  $\omega_{pe}/\Omega_{ce}$  as a function of  $L$  in different MLT sectors (blue: 00-06MLT, green: 06-12MLT, red: 12-18MLT, black: 18-24 MLT) and  $\omega_{pe}/\Omega_{ce}$  based on the statistical plasma density model from (Ozhogin et al., 2012) is shown by dotted black curves. (f-j) 1-MeV electron lifetimes calculated with the actual  $\omega_{pe}/\Omega_{ce}$  (black solid curves) or making use of the model by Ozhogin et al.,(2012)(dotted curves). Exact lifetime values obtained from full numerical calculations are shown by crosses. (k-o) ratio  $\tau/\tau_{Ozh}$  (Agapitov et al., 2020)

# The HISS model – 1 MeV electrons lifetime

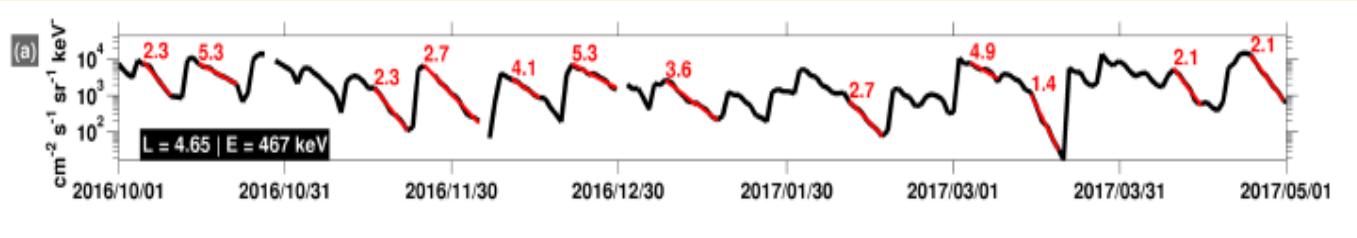


(a) 1-MeV electron lifetime of 1 MeV electrons in the  $L^*$  and  $AE$ -index domain, calculated from  $D\alpha$  distributions obtained from Van Allen Probes measurements. (b) Corresponding 1MeV electrons lifetime parametrization (Agapitov et al., 2020).

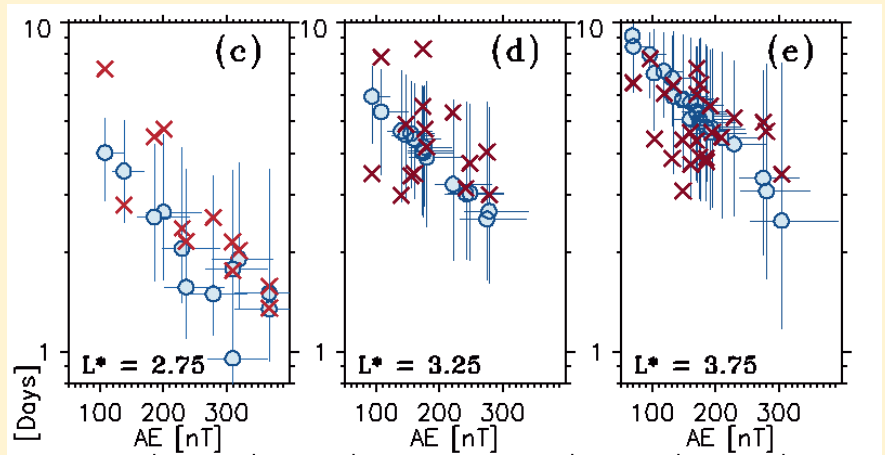


(f) The model values of 1 MeV lifetime for different levels of geomagnetic activity ( $AE$  from 0 to 1000 nT, indicated by curves colors).

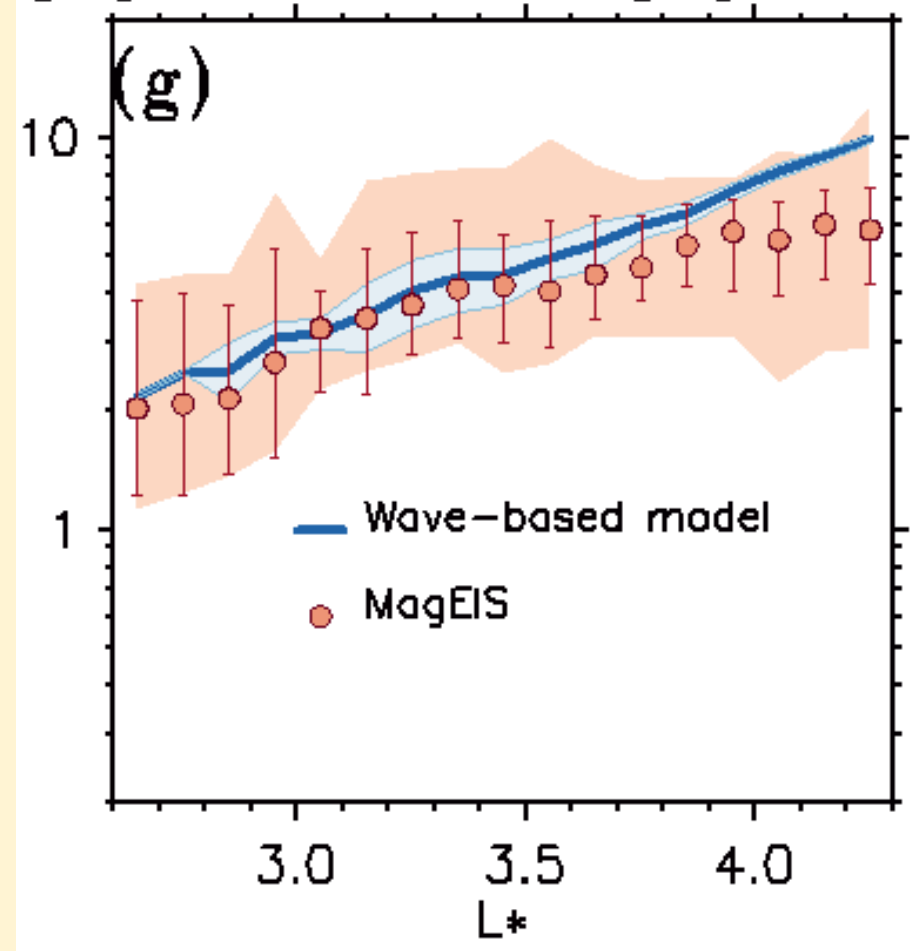
# The HISS model verification



Daily-averaged, differential flux at  $L = 4.65$  for 467-keV electrons. Exponential decays identified by the automated algorithm are highlighted in red with the calculated decay (e-folding) times indicated, in days (from Claudepierre et al., (2020a) )



(c-d) Comparison of  $\tau 1MeV$  from the model (blue circles) with direct estimations (red crosses) from Claudepierre et al., (2020a) based on Van Allen Probes MagEIS measurements of electron flux at  $L^*=2.75, 3.25,$  and  $3.75,$  respectively (Agapitov et al., 2019).



(g) Averaged measured lifetime of 1-MeV electrons obtained by Claudepierre et al., (2020a) (red circles showing the mean, bars showing two standard deviations, and red zone the full variation) and model of  $\tau 1MeV$  (blue curve) (Agapitov et al., 2019).

Based on the new findings we provide **the dynamic chorus wave model** (based on the Van Allen Probes and Cluster VLF observations) for processing the wave-particle interactions and the electron populations dynamics in the outer radiation. We show that taking into account that  $\omega_{pe}/\Omega_{ce}$  in the night/morning sector goes down from 3.5 to  $\sim 1.5$  during geomagnetic activity enhancement leads to **(1) decrease the latitudes of electron cyclotron resonance with chorus waves down to  $\sim 15^\circ$  increasing effective wave amplitudes and  $D_{aa}$ ;**  
**(2) increase  $D_{EE}$  leading to fast local acceleration at  $L^* \sim 3.5 - 4.5$  with the time scales 2-3 hours.**

The effects from  $\omega_{pe}/\Omega_{ce}$  variations indicate the needs **to map directly the dynamics of the scattering rates, i.e. naturally involve all the discussed effects into the models .**

The successful use of this approach we demonstrate providing the **parameterization of MeV electrons lifetimes due to hiss-driven pitch-angle scattering inside the plasmasphere.** The plasma- and wave-based lifetimes are in good agreement with recent measured electron lifetimes from the Van Allen Probes (Claudepierre et al., 2020a) in the region of efficient electron scattering by hiss waves (from  $L^* \sim 2.6$  up to the plasmopause) between  $L^* = 2.6$  and  $L^* = 3.9$  for  $AE = 0$  up to 400 nT at least, and can explain the behavior of 1-MeV electrons in the  $L^*$  range from 2.6 to 3.5-3.9, and it can be used as a realistic estimation of hiss contribution to electron precipitation rates above  $L^* = 3.8$ .